Supporting information

Computational insight on the origin of unexpected contrast in chiral markers as revealed by STM

Ana Sanz-Matías,*[a] Oleksandr Ivasenko,[b] Yuan Fang,[b] Steven De Feyter,[b] Kazukuni Tahara,[c,d] Yoshito Tobe,[c,e] and Jeremy N. Harvey*[a]

December 1, 2017

Contents

[a] *Quantum Chemistry and Physical Chemistry, Department of Chemistry, KU Leuven, BE-3001 Heverlee, Belgium; E-mail: jeremy.harvey@kuleuven.be, ana.sanzmatias@kuleuven.be*
[b] *Molecular Imaging and Photonics Section, Department of Chemistry, KU Leuven, BE-3001 Heverlee, Belgium.*
[c] *Division of Frontier Materials Science, Graduate School of Engineering Science, Osaka University, Toyonaka, Osaka 560-8531, Japan*
[d] *Department of Applied Chemistry, School of Science and Technology, Meiji University, Kawasaki, Kanagawa 214-8571, Japan*
[e] *The Institute of Scientific and Industrial Research, Osaka University, Ibaraki, Osaka 567-0047, Japan*

S1 Details of STM experimental images

The experimental STM images in Figures 1 and 6 were obtained at room temperature, in constant-current mode at sample-negative bias (i.e., tunneling current flowing from the sample to the tip). The specific imaging parameters (bias voltage, V, and tunneling current, I_{set}) are indicated in each figure caption. STM tips were mechanically cut from Pt/Ir wire (80/20, diameter 0.25 mm). The solvent used was commercial 1-phenyloctane. For general details on the procedure, see Ref.[1] for images in Figure 1 and Figure 6 (top); and Ref.[2] for the images in Figure 6 (bottom).

S2 Gaussian input example for 4-methyloctane on graphene flake (with coordinates)

Typical Gaussian 09 100PBE single-point input, in this case for 4-methyloctane on a graphene flake. The formatted checkpoint file contains the data needed to obtain the orbital cube files. Keeping the original orientation of the coordinates (i.e. the graphene parallel to the xy plane) makes easier the postprocessing of the cube files to obtain the STM images. Hence the nosymm keyword, which prevents the reorientation into standard coordinates. The IOp keywords indicate the use of 100% Hartree-Fock exchange instead of PBE.

```
%chk=4mo-100pbe-H.chk
#P sp formcheck nosymm PBEPBE IOp(3/76=0000010000) IOp(3/77=0000000000) 6-311G*

100PBE single-point of 4-methyloctane on a graphene flake

0 1
C     -23.506443   8.413595    3.495133
C     -22.305207   9.363062    3.571506
H     -23.636663   7.868391    4.430195
H     -23.382990   7.680053    2.699381
H     -24.426827   8.964352    3.298845
C     -20.976358   8.611677    3.760406
C     -19.717774   9.506961    3.740546
C     -18.452981   8.620108    3.768481
C     -17.122984   9.385033    3.656238
C     -15.912232   8.444216    3.577010
C     -14.581780   9.204147    3.531577
C     -19.727755   10.531569   4.891981
H     -22.470945   10.058352   4.393590
H     -22.258480   9.966274    2.665827
H     -20.889814   7.869015    2.965539
H     -21.009527   8.047413    4.693509
H     -19.715142   10.061006   2.800951
H     -18.507729   7.905960    2.945264
H     -18.446959   8.023092    4.681530
H     -16.995582   10.038237   4.518941
H     -17.144918   10.031540   2.778678
H     -15.998639   7.808760    2.696039
H     -15.910611   7.772707    4.436461
H     -14.559103   9.913665    2.705250
H     -13.744299   8.517745    3.403443
H     -14.416564   9.764131    4.452302
H     -18.867856   11.198534   4.847898
H     -19.718877   10.037723   5.863988
H     -20.604361   11.176544   4.853480
H     -0.297626    0.163887    0.000000
C      0.000000    2.840000    0.000000
        ...
H     -31.973658   -1.090000   0.000000
H     -31.973658   25.230000   0.000000
```

S3 LDOS integration code

```
program cube_to_ldos
!Ana Sanz-Matias, Mar 2017
!Program that reads a Molecular Orbital cube file (e.g, from gaussian) and transforms
!it in integrated local density of states, iLDOS(x,y,V) by sum(|MO_1|^2 + |MO_2|^2..)
! to be read by plstm.x. The x, y, z values are in bohrs.
!COMPILE: gfortran cube_to_ldos.f90 -o cube_to_ldos.x
!INLINE INPUT:
! number of cube files to be integrated (n), cube file 1, cube file 2, ... cube file n.
!RUN: cube_to_ldos.x < n {1}.cube {2}.cube .... {n}.cube
implicit none
integer :: i, line, k, j, ninputs, cubeinput, natoms, mesh(3)
double precision :: voxel(3,3), valn
double precision, allocatable :: val(:,:,:), valnew(:,:,:)
character(50) :: filename, cubes(20)
!Read number of inputs and filenames
ninputs=iargc()
do i=1, ninputs
   call getarg(i, cubes(i))
enddo
write(*,*) 'number␣of␣inputs', ninputs !Check
write(*,*) (cubes(i),i=1,ninputs) !Check
!Read the cube files data:
do cubeinput=1, ninputs
    open(unit=cubeinput, file=(cubes(cubeinput)))
   !Read cube file header:
    read(cubeinput,*)
    read(cubeinput,*)
    read(cubeinput,*) natoms
    !x=rows,y=columns
    do i=1,3
      read(cubeinput,*) mesh(i) , (voxel(i,k),k=1,3)
    enddo
    do i=1, abs(natoms)+1
     read(cubeinput,*)
```

```
     enddo
    !Allocate charge density matrices (only the first time):
     if (cubeinput .eq. 1) then
       allocate(val(mesh(1),mesh(2),mesh(3)))
       allocate(valnew(mesh(3),mesh(2),mesh(1)))
       valnew=0.d0
     endif
    !keep reading the grid values and reorder them for plstm:
     do i=1,mesh(1)
         do j=1,mesh(2)
             read(cubeinput,*)  (val(i,j,k),k=1,mesh(3))
             !summation: previous value + (new^2)
             do k=1,mesh(3)
                valnew(k,j,i)=valnew(k,j,i)+(val(i,j,k)**2)
             enddo
        enddo
 enddo
enddo
!Write output in LDOS format for plstm.x:
write(filename,'(i2,a)') ninputs, 'cubes.LDOS'
open(unit=77, file=filename)
write(77,*) mesh(1)*voxel(1,1), 0.0, 0.0
write(77,*) 0.0, mesh(2)*voxel(2,2), 0.0
write(77,*) 0.0, 0.0,  mesh(3)*voxel(3,3)
write(77,*) mesh(1), mesh(2), mesh(3), 1
do i=1,mesh(3)
      do j=1,mesh(2)
          do k=1, mesh(1)
            write(77,"(es12.4)") valnew(i,j,k)
          enddo
     enddo
enddo
endprogram
```

S4 Band structures

The energetics of the electronic structure of graphene, specially close to the Fermi level, is not greatly disturbed by physisorbed adsorbates like the ones studied here. Figure S1 shows a comparative of the band structures of octane, 4-methyloctane and octan-4-ol (top); and MPE-OC_{12}, cMPE-$OC_{12}(S)$ and cMPE-$OC_{12}(S)$-OH (bottom); in both cases on a 12x12 supercell of graphene. The horizontal axes of the plots correspond to the high symmetry points of the graphene supercell Brillouin zone (Γ, K and M). The Dirac point coincides with the Γ point because of the 3Nx3N size of the graphene supercell[3].

These band structures were calculated with SIESTA/PBE, as explained on the Computational Methods. In both cases, the main difference with respect to the band structure of the pristine graphene lies in the presence of electronic states localized on the adsorbed molecules. For instance, the highest occupied states localized in the molecules ("HOMOs") of octane, 4-methyloctane and octan-4-ol can be distinguished on the top diagram as the orange, blue and green horizontal lines at -6.98, -6.92 and -5.73 eV, respectively. The HOMO of octan-4-ol is no longer delocalized along the σ-skeleton of the alkylic chain, but localized on the hydroxyl substituent (Fig. S11), hence the difference in energy. The HOMOs of MPE-OC_{12} and its derivatives are localized in the aromatic ring and thus are higher in energy, closer to the Fermi level of graphene.

The following band plots compare, for tDBA-OC_7, tcDBA-$OC_7(R,S)$ and tcDBA-$OC_7(R,S)$-OH, the electronic structures of the molecules in the gas phase, the pristine graphene, and the adsorbate systems. Since the size of the graphene supercell is 16x16 (and not 3Nx3N), the Dirac point coincides again with the K point of the supercells' Brillouin zone. For these systems, the highest occupied state localized in the molecule lies very close to the Fermi level of the graphene in the K point. Hence the brightness of the aromatic region even at small values of the bias voltage.

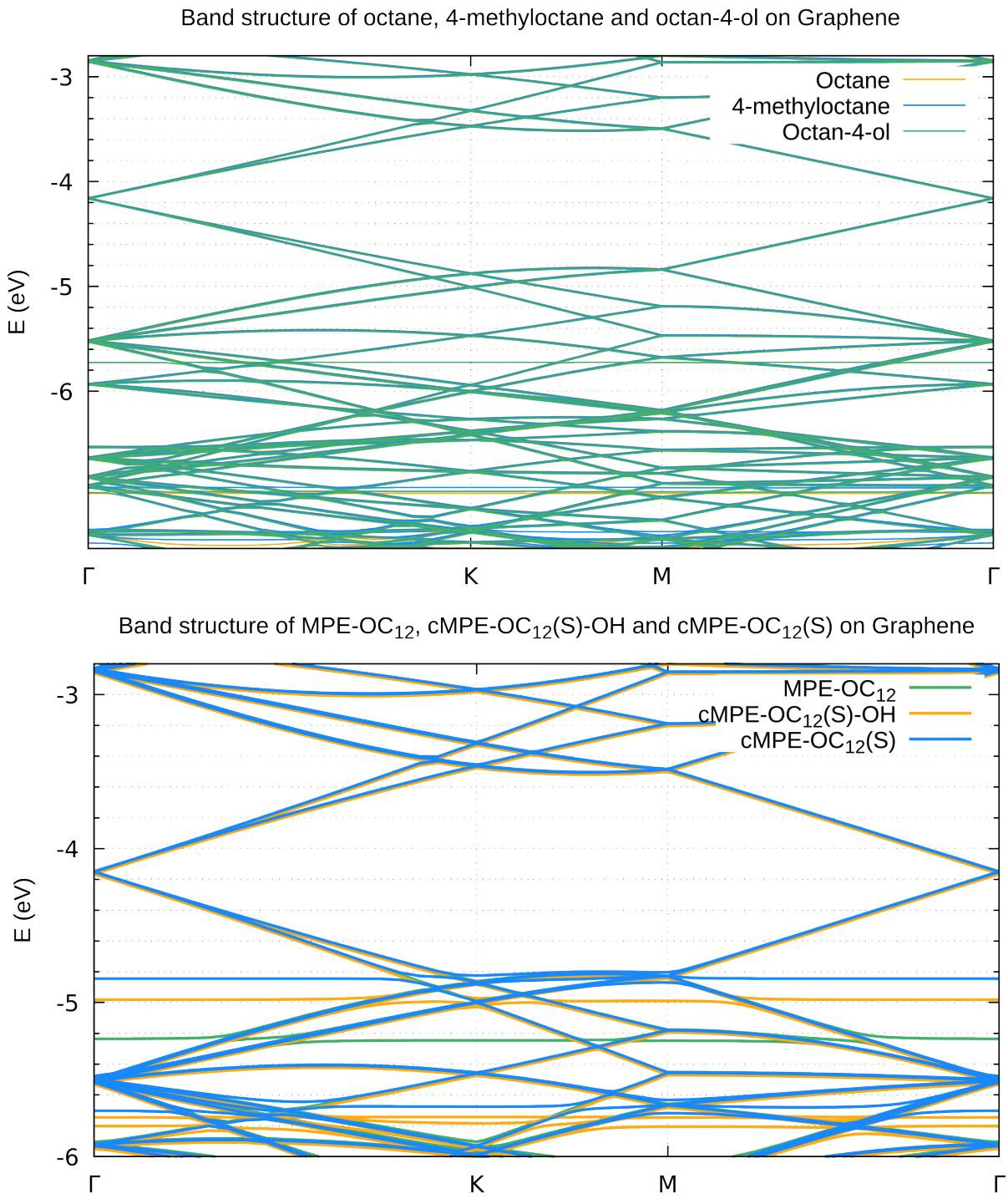

Figure S1: SIESTA band structures of octane, 4-methyloctane and octan-4-ol on periodic graphene calculated with PBE (as per the main text Computational Methods.

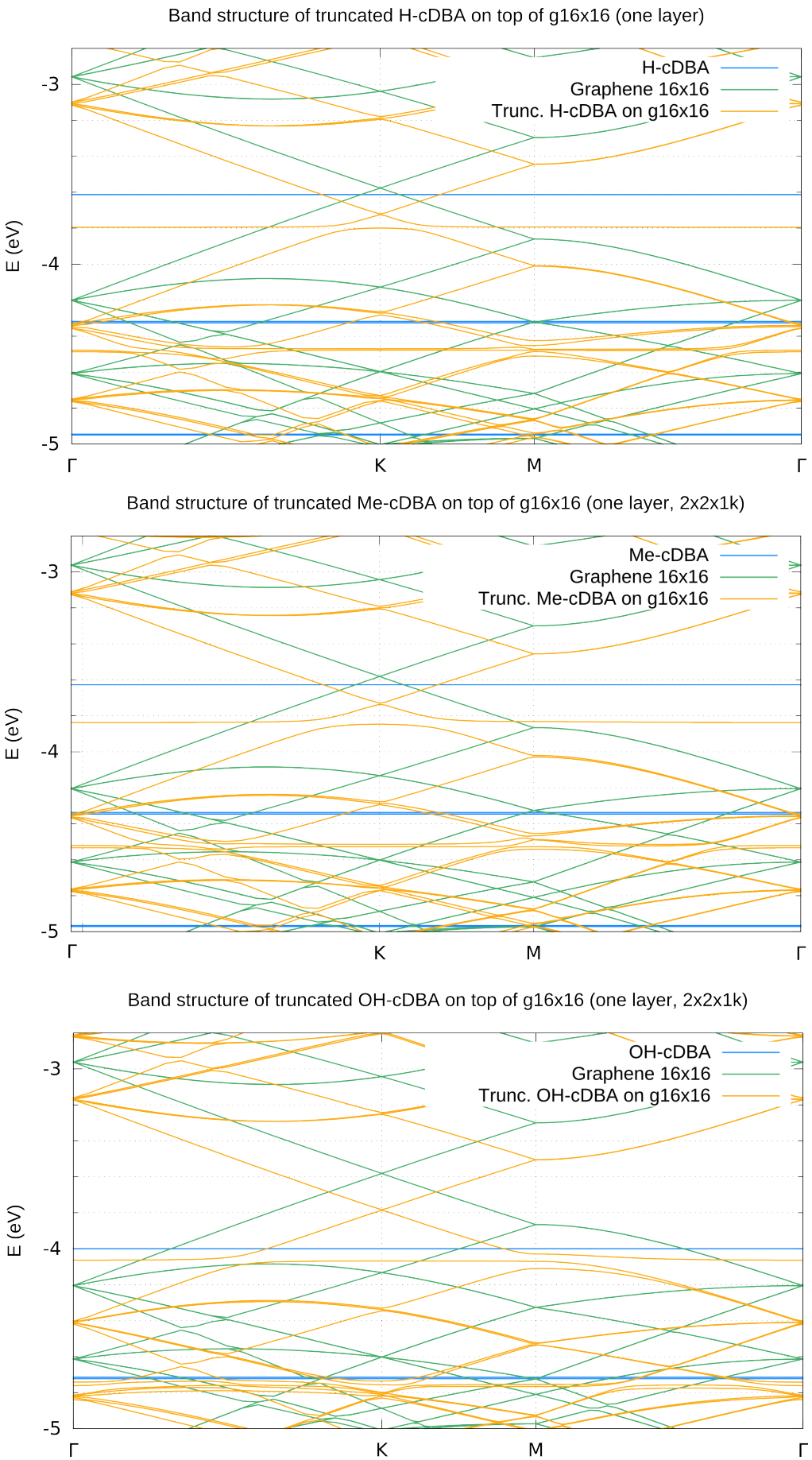

Figure S2: SIESTA band structures of tDBA-OC_7, tcDBA-$OC_7(R,S)$ and tcDBA-$OC_7(R,S)$-OH on periodic graphene calculated with PBE (as per the main text Computational Methods.

S5 Adsorption energies

We calculated the adsorption energies of all the molecules in Scheme 1 and the two possible orientations (up and down). The adsorption energy in each case is taken as:

$$E_{adsorption} = E_{adsorbate} - E_{two-layer\ graphite} - E_{molecule_{(g)}}$$

Each geometry was optimized separately as explained in the computational methods. Since these are Molecular Mechanics total and adsorption energies, we take them merely as a qualitative indicator of the adsorption orientation preference.

Adsorbate	E_T	E_{ads}
octane	-13.93	-16.85
4-methyloctane (up)	-11.81	-17.34
4-methyloctane (down)	-10.15	-16.20
octan-4-ol (up)	-20.12	-17.17
octan-4-ol (down)	-20.01	-17.36
MPE-OC_{12}	-26.65	-39.02
cMPE-OC_{12} (up)	-23.73	-39.69
cMPE-OC_{12} (down)	-20.73	-38.00
cMPE-OC_{12} (OH,up)	-28.14	-39.38
cMPE-OC_{12} (OH,down)	-27.85	-39.32
tcDBA-OC_7 (up)	-46.27	-80.48
tcDBA-OC_7 (down)	-39.71	-78.33
tcDBA-OC_7 (OH,up)	-53.33	-79.17
tcDBA-OC_7 (OH,down)	-52.63	-79.32

Table S1: MM OPLS-AA total energies (E_T) and adsorption energies (E_{ads}) in kcal/mol of different adsorbates on periodic two-layered graphite

S6 STM simulated images

S6.1 Comparison of PBE and 100PBE STM simulated images of octane

STM images of octane calculated with the PBE and 100PBE functionals (as indicated in the Computational Methods) are substantially similar. The (lack of) octane features follows a similar trend with bias voltage in both cases.

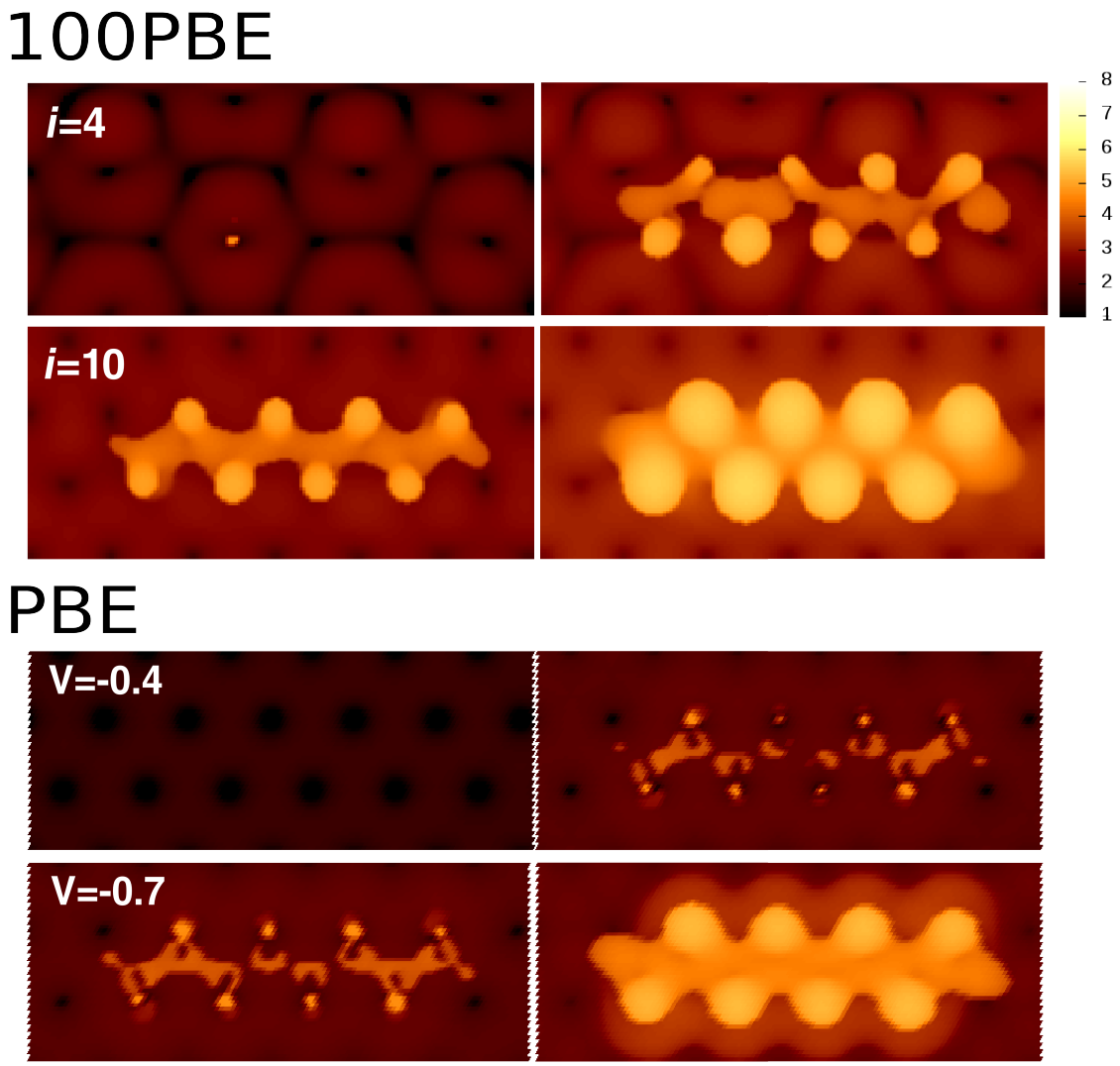

Figure S3: Comparison of STM images of octane with PBE and 100PBE (as per Computational Methods in the Computational Methods) at iLDOS=10^{-6} (left) and 10^{-7} (right) e bohr^{-3}. The number of integrated orbitals is indicated by i. The color scale represents height (1 to 8 Å).

S6.2 Effect of the graphene layer

Figure S4 shows a series of STM simulated images of 4-methyloctane at calculated at increasing values of the bias voltage with one and two-layered graphene in AB stacking. The size of the graphene supercell is 12x12. These images were calculated calculated with the PBE functional, as explained in the Computational Methods. We can see that the marker (lack of) features remain essentially constant independently of the number of graphene layers considered here. The exception are, specially, the STM images calculated at V=−0.1 (top row in Fig. S4). The second graphene layer introduces two extra degenerate occupied bands besides the already existing two, which lay very close to the Fermi level in the Dirac point.* Hence, two more states can contribute to the tunneling. This difference is significant and noticeable only at very small bias voltages when only a few states fall within the relevant energy range for the tunneling, as is the case in these particular images.

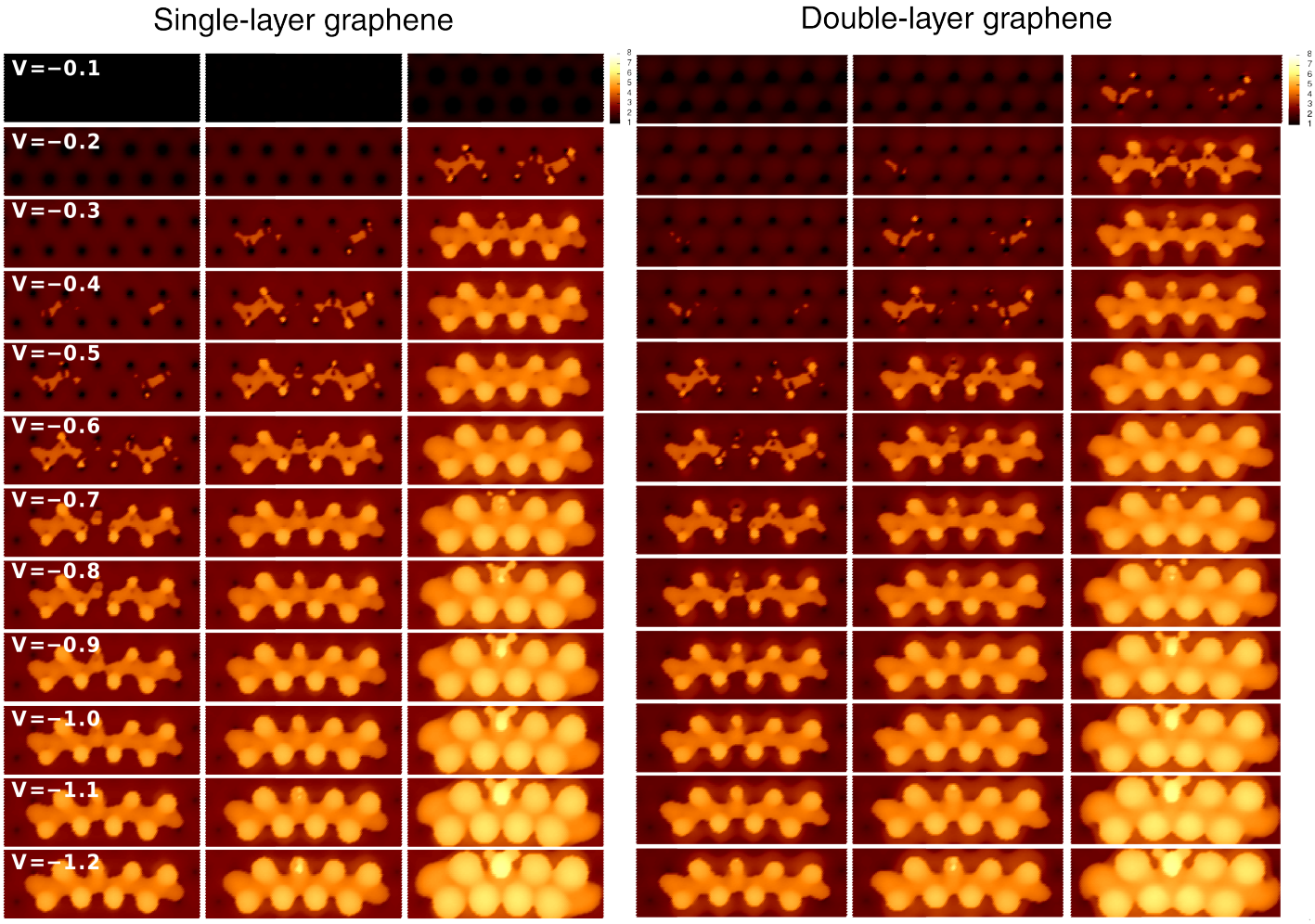

Figure S4: Comparison of STM images of 4-methyloctane with calculated with the PBE functional at iLDOS=10^{-6} (left), 5 10^{-6} (center) and 10^{-7} (right) e bohr^{-3} with one and two-layered AB-stacked graphene. The color scale represents height (1 to 8 Å).

*For 3N supercells, as is this case (12x12), the Dirac point coincides with the Γ instead of with the K point.[3]

S6.3 Effect of bias polarity in simulated images of 4-methyloctane

Images of 4-methyloctane are largely independent on the polarity of the bias voltage, within the enrgy range of interest in this study.

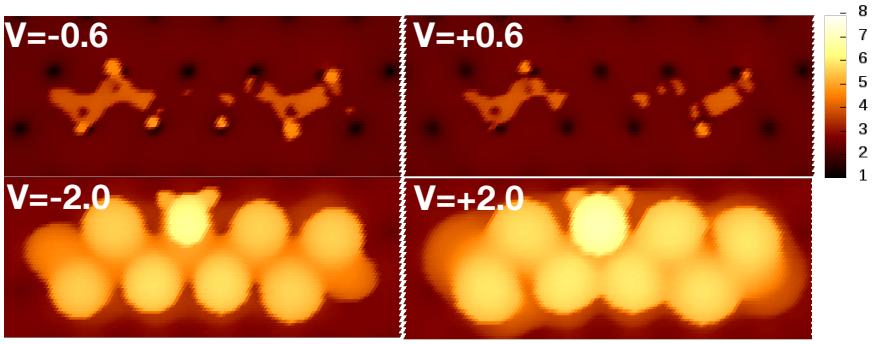

Figure S5: STM images of 4-methyloctane at iLDOS=10^{-6} e bohr^{-3} calculated at bias voltages V=-0.6, +0.6, -2.0 and +2.0 V. The color scale represents height (1 to 8 Å).

S6.4 STM simulated images of 4-methyloctane with 100PBE

STM images of 4-methyloctane calculated with the 100PBE functional (Fig. S3) are substantially similar to the ones calculated with the PBE functional (Fig. S4). The (lack of) marker features is very similar in both cases, and follows a similar trend with bias voltage increase.

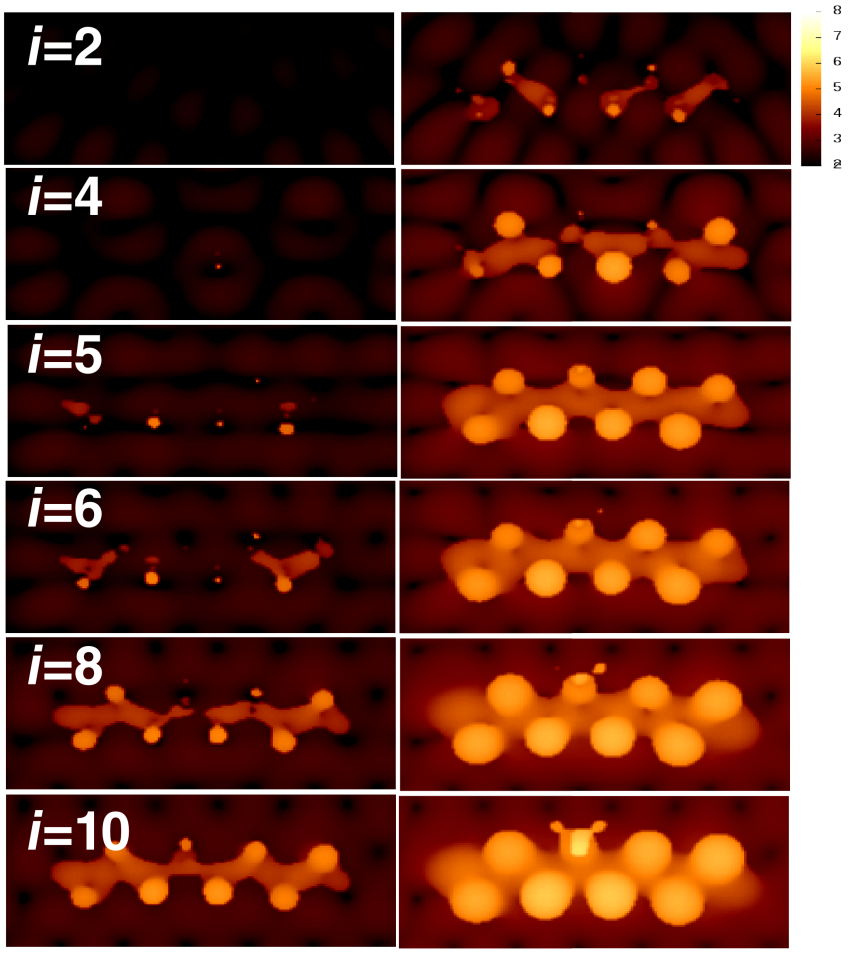

Figure S6: Comparison of STM images of 4-methyloctane 100PBE (as per Computational Methods in the Computational Methods) at iLDOS=10^{-6} (left) and 10^{-7} (right) e bohr^{-3}. The number of integrated orbitals is indicated by i. The color scale represents height (1 to 8 Å).

S6.5 Comparison of PBE and 100PBE STM simulated images of octan-4-ol

For octan-4-ol, the marker features differ slightly between the images calculated with the PBE and the 100PBE functionals (Fig. S7). As commented in the main text, the HOMO in the 100PBE calculations is less localized in the oxygen atom (Fig. S11) and hence the marker appears less bright at small (i=4 vs V=-0.4) bias voltages. The difference at larger bias voltages (i=14 vs V=-2.0) may be a consequence of the greater localization of the charge density due to the use of the 100PBE functional. Furthermore, the highest occupied state localized mainly on the molecule is higher in energy in the PBE calculations, possibly due to their periodic nature. Hence, this state can contribute to the tunneling. In the case of the 100PBE calculations, the âHOMOâ is outside this range and can contribute to the tunnelling only through admixture with other orbitals. As a result of both factors, the area of the image corresponding to the molecule appears brighter in the PBE calculated images.

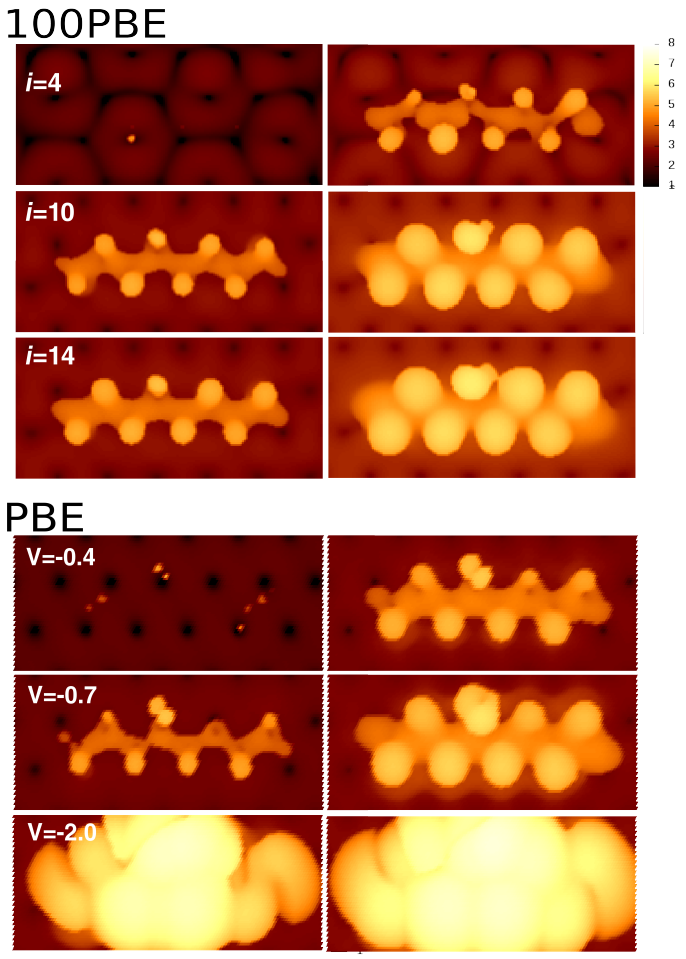

Figure S7: Comparison of STM images of octan-4-ol with 100PBE and PBE (as per Computational Methods in the Computational Methods) at iLDOS=10^{-6} and 10^{-7} e bohr^{-3}. The number of integrated orbitals is indicated by i. The color scale represents height (1 to 8 Å).

S6.6 Sideview of the STM images of octane, 4-methyloctane and octan-4-ol

A sideview of the STM simulated images of octane, 4-methyloctane and octan-4-ol on graphene is shown in Fig. S8. These images were calculated with PBE/SIESTA, as described in the Computational Methods. The superposition of small (V=-0.6) and large (V=-2.0) bias voltages allows to compare the depth of the 'dark spot' in 4-methyloctane (central plot). Interestingly, the large bias voltage isosurface of octan-4-ol is comparatively larger than in the other two adsorbates. This is due to the fact that at V=-2.0, the top occupied state localized in the molecule (i.e., the "HOMO") can contribute to the tunneling, since it lies in the relevant energy range. Hence, the image height is remarkably larger than in the analogous images of octane and 4-methyloctane.

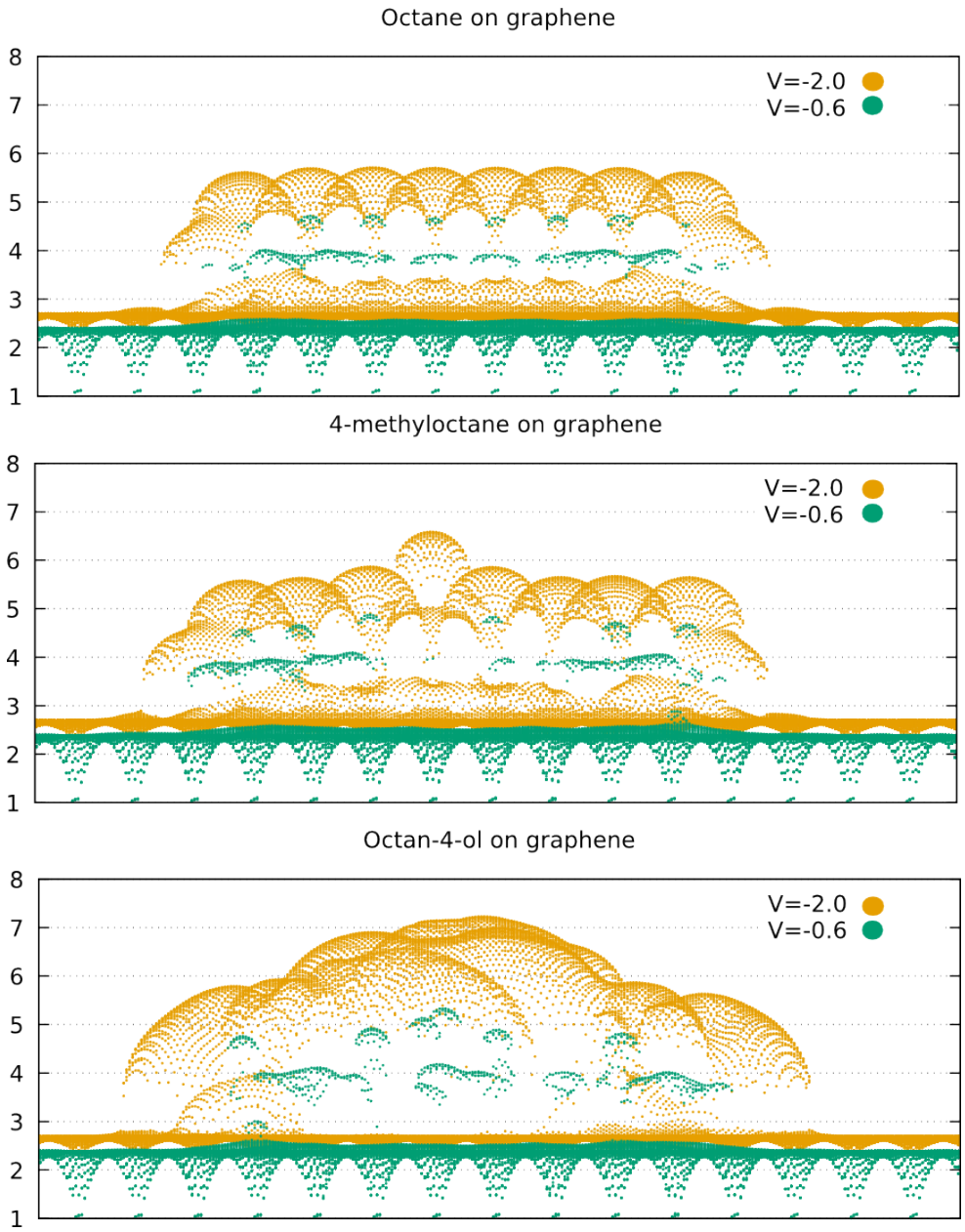

Figure S8: Sideview of the integrated LDOS of octane, 4-methyloctane, and octan-4-ol at iLDOS=10^{-6} e bohr^{-3} and V=-0.6 and -2.0 V. The height is in Å.

S6.7 Effect of the self-interaction errors: marker-aromatic region distance

As mentioned in the main text, self-interaction errors cause an overdelocalization of the electron density in the aromatic ring, which 'leaks' to the nearby regions and makes them appear brighter in the calculated images. To test this effect, with varied the marker-aromatic region distance in two methylated derivatives of MPE-OC_{12}. Figure S9 shows the STM images of 2- and 5-methylated cMPE-$OC_{12}(S)$ (left and right, respectively) calculated with PBE/SIESTA. The marker in 2-cMPE-$OC_{12}(S)$ appears bright already at V=-0.4 (white circle in Fig. S9, left). At a greater marker-aromatic region distance, such as in 5-cMPE-$OC_{12}(S)$, the 'dark spot' reappears (V=-0.2), and the marker becomes fully bright at bias voltages larger than V=-0.6 (white circle in Fig. S9, right). We note that during this investigation, we also tried range-separated functionals, such as ωB97. The results obtained were similar to those of the PBE functional, albeit at a higher computational expense.

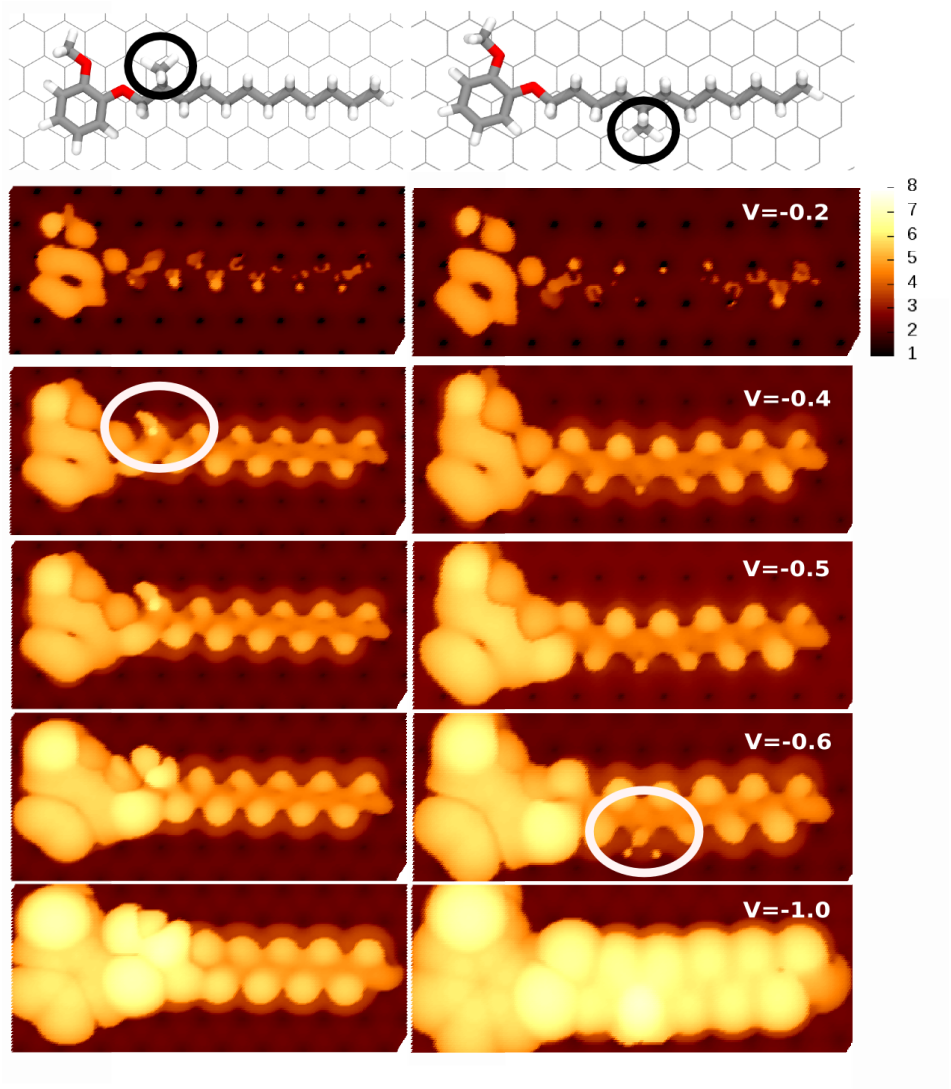

Figure S9: STM images of 2- and 5-cMPE-OC_{12} calculated with SIESTA/PBE at LDOS=10^{-7} e bohr^{-3} and different bias voltages. The color scale represents height (1 to 8 Å).

S6.8 STM simulated images of cMPE-OC$_{12}$(S)-OH calculated with 100PBE

Sample of STM simulated images of cMPE-OC$_{12}$(S)-OH (up) calculated with 100PBE at different bias voltages. The hydroxyl marker starts to appear bright in images at i>9.

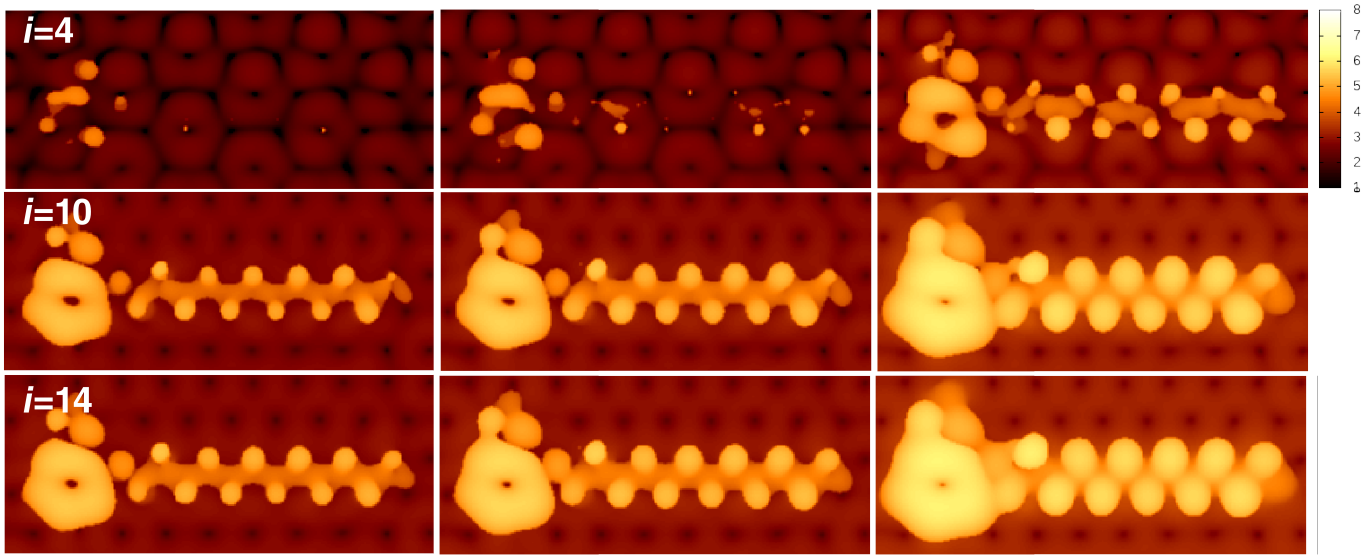

Figure S10: STM images of cMPE-OC$_{12}$(S)-OH calculated with 100PBE (as per Computational Methods in the Computational Methods) at iLDOS=10^{-6}, 5 10^{-6} and 10^{-7} e bohr^{-3}. The number of integrated orbitals is indicated by i. The color scale represents height (1 to 8 Å).

S7 Molecular Orbitals

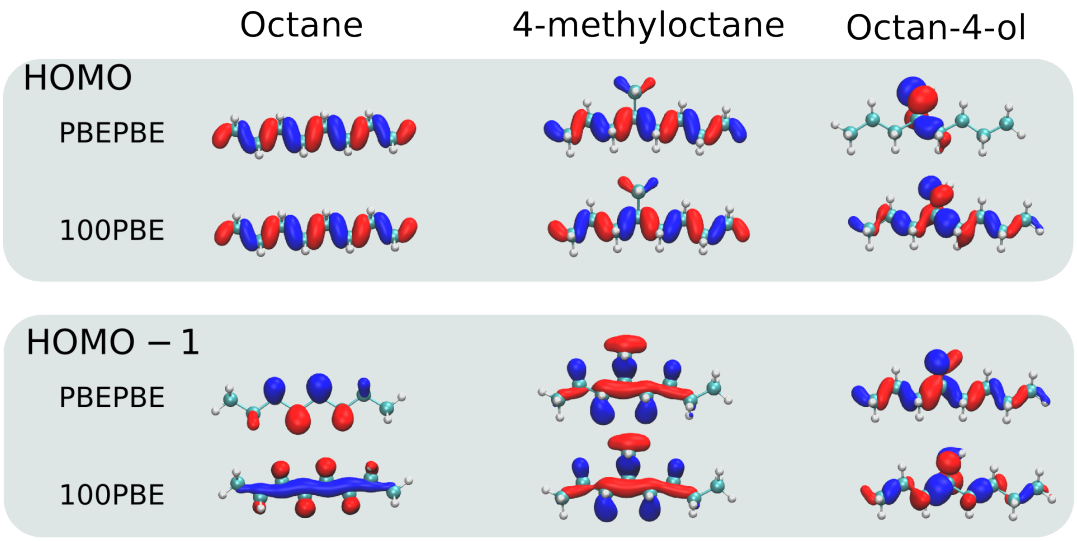

Figure S11: Gas-phase HOMO and HOMO-1 of octane, 4-methyloctane and octan-4-ol calculated with the PBEPBE and 100PBE functionals.

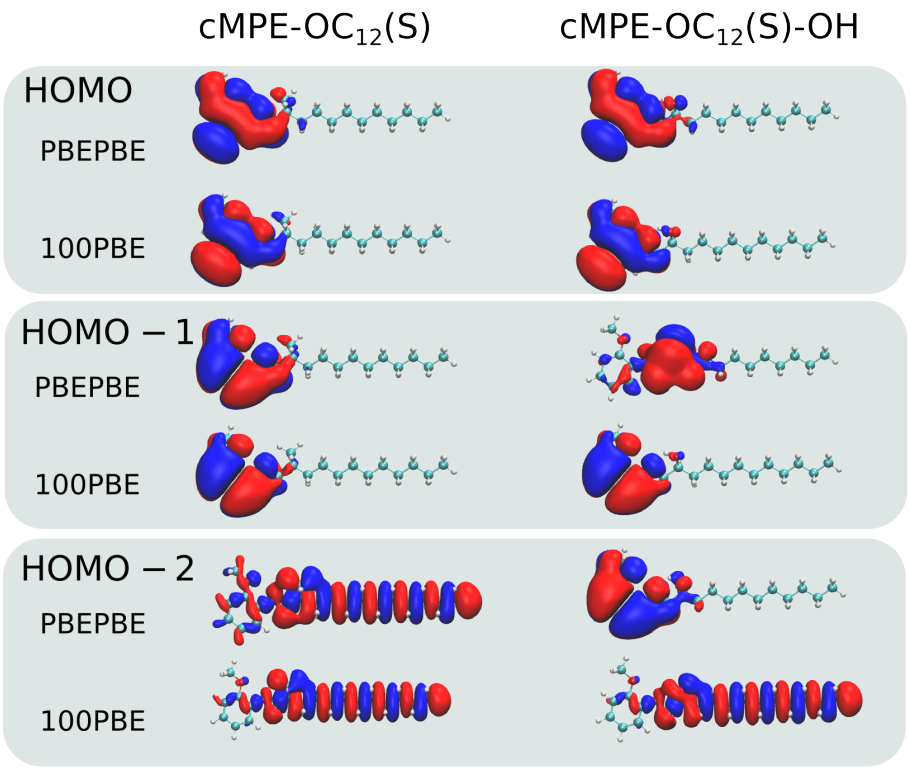

Figure S12: Gas-phase HOMO, HOMO-1 and HOMO-2 of cMPE-$OC_{12}(S)$ and cMPE-$OC_{12}(S)$-OH calculated with the PBEPBE and 100PBE functionals.

S8 Geometries: effect of the method

In this study, a lower level of theory was used for geometry optimization (Molecular Mechanics) than for electronic structure calculations (DFT), as stated in the Computational Methods Section. Here we provide the resulting geometries of some test calculations to justify this choice of computational setup.

As mentioned in the main text, dispersion corrections such as Grimme's D2 or D3 are not implemented in SIESTA. Furthermore, some of the systems studied here (the chiral DBAs) can easily reach a few hundred atoms when adsorbed on the surface. Force-field optimization becomes, hence, an efficient solution for obtaining dispersion-corrected geometries.

The following figure (Fig. S13) shows the optimized geometries obtained for 4-methyloctane on a graphene flake using OPLS-AA force field parameters (black); dispersion corrected DFT (B3LYP-D3, in green, and PBE-D3, in red); and uncorrected DFT (PBE, in orange). The graphene flake is kept frozen. The similarity between the calculations including dispersion contrasts with the larger surface-molecule distance present in the PBE optimized structure. RMSD values with respect to the OPLS-AA geometry are: 0.068 Å (B3LYP-D3), 0.033 Å (PBE-D3), and 0.27 Å (PBE). If we only account for the molecule in the RMSD calculation, however, the values drop to, respectively, 0.039, 0.032 and 0.064 Å. The surface-adsorbate distance is, approximately, 0.7 Å smaller for the dispersion-corrected calculations.

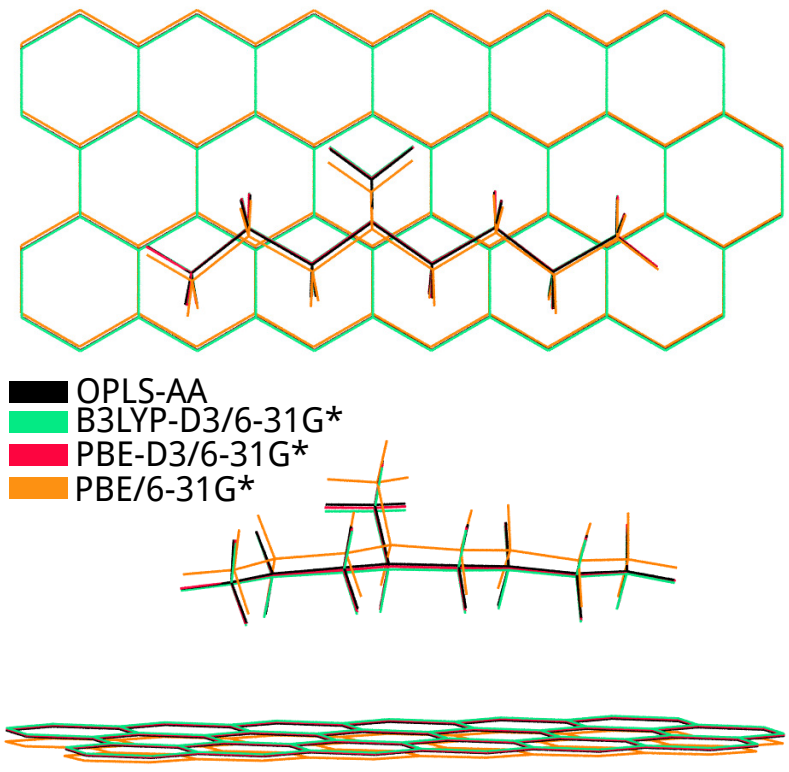

Figure S13: Comparison of 4-methyloctane on a graphene flake geometries optimized with OPLS-AA force field parameters (black); dispersion corrected DFT (B3LYP-D3, in green, and PBE-D3, in red); and uncorrected DFT (PBE, in orange); top and side view. The hydrogen atoms in the graphene flake edges are not shown for clarity.

On the other hand, the lack of dispersion correction in the electronic structure SIESTA calculations leads to relatively large atomic forces, which are, however, artifacts. For instance, for 4-methyloctane on one graphene layer, the largest force amounts to 1.1 eV/Å. To test the robustness of our calculated images, we performed a series of STM calculations in which

the surface-molecule distance was varied, while maintaining the internal molecular structure rigid. The results are shown in Fig.S14. Unsurprisingly, the choice of bias voltage and iLDOS, as well as the molecule-surface distance, strongly affect contrast in the calculated images. The 'dark spot', nonetheless, persists.

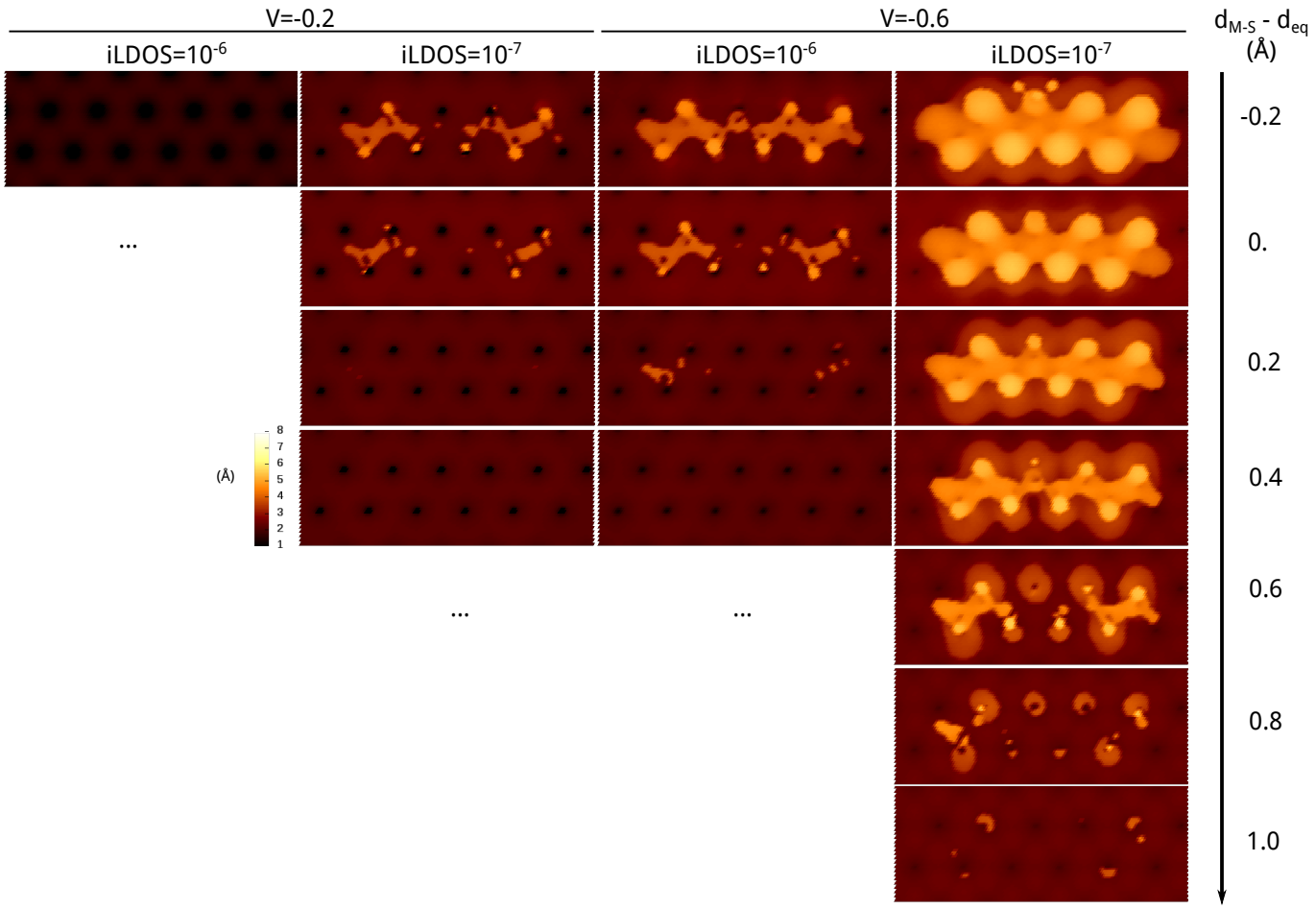

Figure S14: Images of 4-methyloctane on graphene calculated with SIESTA at bias voltages V=-0.2 and V=-0.6. The (rigid) variation of the surface-molecule distance ($d_{M-S} - d_{eq}$) is shown on scale in the right side of the images. The ellipses indicate that the following images are identical to the one above. Images at $d_{M-S} - d_{eq} = 0$ correspond to the OPLS-AA equilibrium structure, while images at $d_{M-S} - d_{eq}$ values below or above zero correspond to the artificially modified structures (closer or further from the surface).

References

[1] Yuan Fang, Elke Ghijsens, Oleksandr Ivasenko, Hai Cao, Aya Noguchi, Kunal S. Mali, Kazukuni Tahara, Yoshito Tobe, and Steven De Feyter. Dynamic control over supramolecular handedness by selecting chiral induction pathways at the solutionâsolid interface. *Nature Chemistry*, 8(7):711–717, 2016.

[2] Kazukuni Tahara, Hiroyuki Yamaga, Elke Ghijsens, Koji Inukai, Jinne Adisoejoso, Matthew O. Blunt, Steven De Feyter, and Yoshito Tobe. Control and induction of surface-confined homochiral porous molecular networks. *Nature Chemistry*, 3(9):714–719, 2011.

[3] Ye-Cheng Zhou, Hao-Li Zhang, and Wei-Qiao Deng. A 3 N rule for the electronic properties of doped graphene. *Nanotechnology*, 24(22):225705, 2013.